Tuning Magnesium Sensitivity of BK Channels by Mutations

Huanghe Yang, Lei Hu, Jingyi Shi, and Jianmin Cui
Department of Biomedical Engineering and Cardiac Bioelectricity and Arrhythmia Center, Washington University, St. Louis, Missouri 63130

ABSTRACT   Intracellular Mg^{2+} at physiological concentrations activates mSlo1 BK channels by binding to a metal-binding site in the cytosolic domain. Previous studies suggest that residues E374, Q397, and E399 are important in Mg^{2+} binding. In the present study, we show that mutations of E374 or E399 to other amino acids, except for Asp, abolish Mg^{2+} sensitivity. These results further support that the side chains of E374 and E399 are essential for Mg^{2+} coordination. To the contrary, none of the Q397 mutations abolishes Mg^{2+} sensitivity, suggesting that its side chain may not coordinate to Mg^{2+}. However, because Q397 is spatially close to E374 and E399, its mutations affect the Mg^{2+} sensitivity of channel gating by either reducing or increasing the Mg^{2+} binding affinity. The pattern of mutational effects and the effect of chemical modification of Q397C indicate that Q397 is involved in the Mg^{2+}-dependent activation of BK channels and that mutations of Q397 alter Mg^{2+} sensitivity by affecting the conformation of the Mg^{2+} binding site as well as by electrostatic interactions with the bound Mg^{2+} ion.

INTRODUCTION

BK-type K^+ channels are activated by voltage and intracellular Ca^{2+}. This unique property of the BK channel activation makes it important in physiological processes in various cell types (1–15). Because BK channels have a large single-channel conductance, their opening hyperpolarizes membranes with high efficiency, resulting in the closure of voltage-dependent Ca^{2+} channels and hence decreasing $[Ca^{2+}]_i$. Thus, BK channels provide a negative feedback in controlling the membrane potential and $[Ca^{2+}]_i$. Based on this mechanism, BK channels modulate various physiological processes including neural excitation (5,11,16–19), muscle contraction (8,15,20–23), hearing (24–27), and immunity (28).

Apart from Ca^{2+}, the function of BK channels is also modulated by intracellular Mg^{2+} (29–40). Mg^{2+} modulates a variety of Ca^{2+} and K^+ channels to affect the excitability or excitation-contraction coupling in neurons, cardiac myocytes, and smooth muscle cells (41–47). Following central nervous system injury, $[Mg^{2+}]_i$ is significantly reduced, contributing to a number of factors including neurotransmitter release and oxidative stress that initiate an autodestructive cascade of biochemical and pathophysiological changes, known as secondary injury, that ultimately result in irreversible tissue damage (48). Pharmacological studies have shown that Mg^{2+} may be an effective therapeutic agent following neurotrauma to improve survival and motor outcome and to alleviate cognitive deficits (48). Magnesium supplements are also important in the prevention and management of cardiovascular diseases that predispose to hypertension or congestive heart failure (49,50). Because of the importance of BK channels in neurotransmitter release and vascular tone, Mg^{2+} modulation of BK channels may play a substantial role in these pathophyisological processes.

BK channels are encoded by *Slo1* genes (51–56) and possess common structural features of voltage-gated K^+ channels. Each Slo1 protein contains a pore domain formed by S5-S6 transmembrane segments and a voltage-sensing domain formed by S0-S4 transmembrane segments (Fig. 1). In addition, a long cytosolic carboxyl terminus forms the Ca^{2+} and Mg^{2+} sensing module (57), which may adopt a similar structure as the cytosolic domain of the K^+ channel in *E. coli* and an *archeon* Ca^{2+}-activated K^+ channel, MthK (58,59). Previous studies have shown that site-directed mutations of mSlo1 E374A, E399N, and Q397C either abolish or reduce Mg^{2+} sensitivity of channel activation (38,40). In models based on the x-ray crystallographic structures of the K^+ channel in *E. coli* (38) and of MthK, these three residues locate closely (Fig. 1) and can form a metal-binding site (38). However, the roles of these residues in Mg^{2+} sensitivity, such as whether they are the ligands for the Mg^{2+} binding site, and how the mutations E374A, E399N, or Q397C affected Mg^{2+} sensitivity are not clear. On the other hand, the putative Mg^{2+} binding site formed by these residues is located in the cytosolic domain, whereas the activation gate is located in the membrane-spanning domain (Fig. 1). The structural separation between the binding site and the activation gate indicates that Mg^{2+} binding activates the channel by an allosteric mechanism; i.e., Mg^{2+} binding may cause a conformational change at the binding site that propagates to the activation gate for channel opening. Such conformational changes have not been explored.

In this study we mutated each of the three residues, E374, E399, and Q397, into amino acids of different chemical properties and examined the activation of mutant channels. We found that mutation of E374 or E399 to any amino acid except Asp abolishes Mg^{2+} sensitivity, a result that is consistent with these two residues being the ligands for the Mg^{2+} binding site. However, none of the mutations of Q397
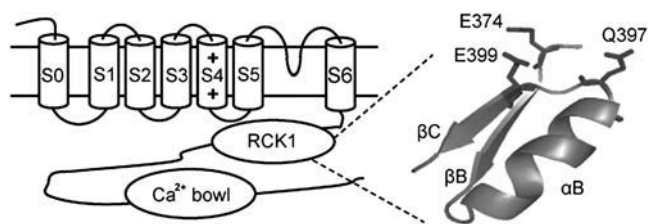
FIGURE 1 Schematic diagram of the α subunit of BK channels (*left*) and the homology model of the Mg^{2+}-binding site of mSlo1 channels based on the crystal structure of the MthK channel (58).

abolished Mg^{2+} sensitivity. Rather, Mg^{2+} sensitivity decreased when Q397 is mutated to neutral or positively charged residues, whereas it increased when Q397 is mutated to negatively charged residues. These results suggest that the side chain of Q397 may not be the ligand for the binding site but is close to the binding site so that the Mg^{2+} sensitivity of channel activation can be tuned by mutating Q397 into different amino acids. We also studied the chemical modification of Q397C mutant channels. The results suggest that the mutations alter Mg^{2+} sensitivity by affecting the conformation of the Mg^{2+} binding site as well as by electrostatic interactions.

MATERIALS AND METHODS

Clones, mutagenesis, and channel expression

All channel constructs were made from the mbr5 clone of mSlo1 (60) using PCR with Pfu polymerase (Stratagene, La Jolla, CA). The PCR-amplified regions of all mutants were verified by sequencing. RNA was transcribed in vitro with T3 polymerase (Ambion, Austin, TX). We injected 0.05–50 ng of RNA into each *Xenopus laevis* oocyte 2–6 days before recording.

Electrophysiology

Macroscopic currents were recorded from inside-out patches formed with borosilicate pipettes of ~1–2 MΩ resistance. Data were acquired using an Axopatch 200-B patch-clamp amplifier (Axon Instruments, Sunnyvale, CA) and pulse acquisition software (HEKA Electronik, Southboro, MA). Records were digitized at 20-μs intervals and low-pass filtered at 10 kHz with the 4-pole Bessel filter built into the amplifier. The pipette solution contained the following (in mM): 140 potassium methanesulfonic acid, 20 HEPES, 2 KCl, and 2 MgCl$_2$, pH 7.20. The basal internal solution contains the following (in mM): 140 potassium methanesulfonic acid, 20 HEPES, 2 KCl, and 1 EGTA, pH 7.20. MgCl$_2$ was added to the internal solution to give the appropriate free [Mg^{2+}]$_i$, and 50 μM 18-crown-6-tetracarboxylic acid (18-C-6-T, Sigma-Aldrich, St. Louis, MO) was added to internal solutions to prevent Ba^{2+} block. Experiments were conducted at room temperature ($\sim$22–24°C).

Structural model

The homology structural model of the mSlo1 channel (βB to βC) based on the crystal structure of the MthK channel (58) was produced using the PyMol molecular graphics system (http://www.pymol.org) (61). E374, Q397, and E399 of the mSlo1 channel correspond to E138, G156, and N158 of the MthK channel. The SWISS-PDB Viewer (62) was used to generate

the corresponding mutant structure by substituting Gln for G156 and Glu for N158 and selecting the lowest-energy rotamer.

Analysis and model fitting

Relative conductance was determined by measuring tail current amplitudes at -50 mV for the WT and mutant mSlo1 channels. The conductance-voltage (*G-V*) relations of the WT and mutant channels were fitted with a Boltzmann equation:

$$\frac{G}{G_{\text{Max}}} = \frac{1}{1 + e^{-ze(V - V_{1/2})/kT}}, \tag{1}$$

where z is the number of equivalent charges, $V_{1/2}$ is the voltage for a channel in half activation, e is the elementary charge, k is Boltzmann's constant, and T is the absolute temperature. For model fittings of E399D, Q397K, Q397E, and Q397C, the *G-V* relations of the mutant channels at various [Mg^{2+}]$_i$ and 0 [Ca^{2+}]$_i$ were fitted with Eq. 2 in Results. Curve fittings were done with Igor Pro software (WaveMetrics, Lake Oswego, OR) using the Levenberg-Marquardt algorithm to perform nonlinear least-squares fits. The means of the data were obtained by averaging from 4 to 16 patches, and error bars represent standard error of means.

Chemical modification

MTSET ([2-(trimethylammonium)ethyl] methanethiosulfonate bromide) was purchased from Toronto Research Chemicals (North York, ON, Canada), dissolved in water at 100 mM, and stored at -80°C. An aliquot of MTSET stock solution was thawed and diluted 500-fold into the appropriate internal solution immediately before use. Currents were recorded after 2.5 min of MTSET treatment and 0.5 min of washing.

RESULTS

We first examined the effects of E374 mutations on the activation of mSlo1 channels. Fig. 2 shows the comparison of the WT mSlo1 activation with that of mutant channels E374R, E374K, E374D, E374A, E374Q, and E374W. It is obvious that the Mg^{2+} sensitivity of mutant E374A is significantly reduced (Fig. 2 *A*). Addition of 10 mM Mg^{2+} resulted in a shift of the *G-V* relation -67.39 ± 1.86 mV for the WT mSlo1 channel but only -12.51 ± 2.60 mV for E374A (Fig. 2 *A*). Our previous studies demonstrated that the channel is activated by two independent Mg^{2+} binding sites, one with high affinity ($K_d = 5.46$ mM when channel is closed and 2.25 mM when channel is open) and the other with low affinity ($K_d = 136.1$ mM when channel is closed and 40.1 mM when channel is open). Mutations of E374, E399, or Q397 affect only the high-affinity binding site but have no effects on the low-affinity site (63). We use a model for channel activation (63) to calculate the amount of the *G-V* shift related to Mg^{2+} binding to the low-affinity site at 10 mM (Eq. 2 and Table 1). This value is then subtracted from the *G-V* shift measured experimentally (*gray bar* in Fig. 2 *C*), which gives rise to the remaining Mg^{2+} sensitivity mediated by the high-affinity Mg^{2+} binding site (*black bar* in Fig. 2 *C*). The result shows that mutation E374A completely abolishes Mg^{2+} sensitivity through the high-affinity Mg^{2+} binding site (Fig. 2 *C*). Fig. 2, *B* and *C*, shows that another mutation,
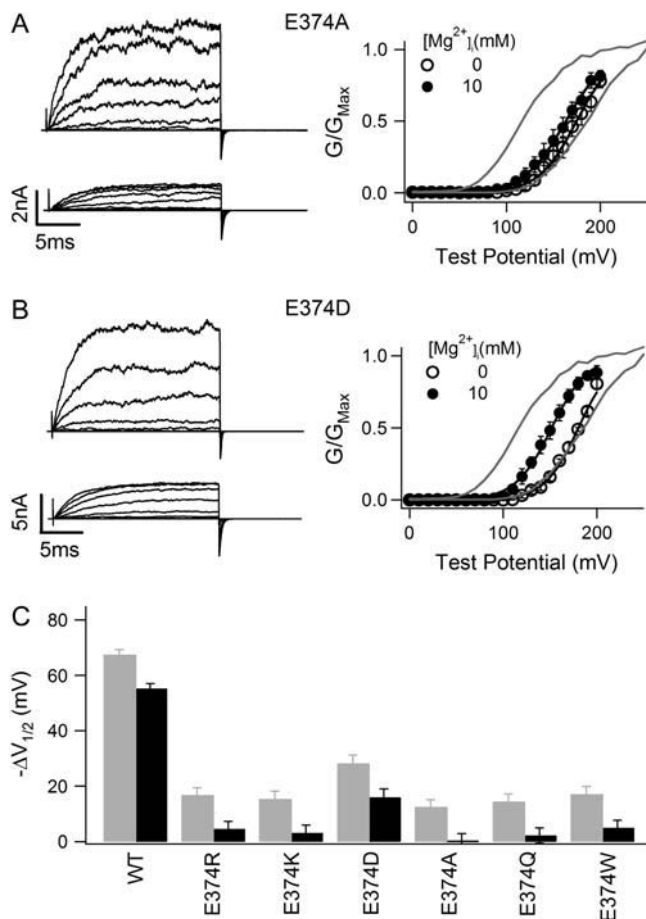
FIGURE 2 Effects of E374 mutations on Mg^{2+} sensitivity. (*A* and *B*) Mg^{2+}-dependent activation of E374A (*A*) and E374D (*B*) channels at 0 $[Ca^{2+}]_i$. (*Left panels*) Current traces recorded at 0 (*upper*) or 10 mM (*lower*) $[Mg^{2+}]_i$. Testing potentials were from −30 to 250 mV with 20-mV increments. The holding and repolarizing potentials were −80 and −50 mV, respectively. (*Right panels*) Mean *G-V* relations. Gray lines are *G-V* relations of WT mSlo1 channels for comparison. *G-V* relations of mutant channels are fitted with the Boltzmann relation (*solid lines*; see Materials and Methods). (*C*) *G-V* shift from 0 to 10 mM $[Mg^{2+}]_i$ at 0 $[Ca^{2+}]_i$ of WT mSlo1 and mutant channels. $V_{1/2}$ is the voltage where the *G-V* relation is half-maximum. Gray bars are the data measured in experiments, and black bars are the experimental data subtracted by the amount of *G-V* shift (−12.2 mV) caused by Mg^{2+} binding to the low-affinity Mg^{2+} site and calculated from model simulation (see Materials and Methods).

E374D, does not entirely abolish Mg^{2+} binding to the site but significantly reduces Mg^{2+} sensitivity. A 10 mM increase in $[Mg^{2+}]_i$ caused a *G-V* shift of −15.95 ± 3.05 mV for E374D even after subtraction of the effect of the low-affinity Mg^{2+} site (Fig. 2 *C*). Among all mutations on E374 that we have studied, only E374D retains Mg^{2+} sensitivity. Other E374 mutations abolish Mg^{2+} sensitivity, similar to E374A (Fig. 2 *C*). Multiple comparison with Tukey's test indicates that the result of E374D in Fig. 2 *C* is significantly different from the result of the other mutants (> 95% confidence level). These results demonstrate that a carboxylate, or negative charge, in the residue at position 374 is essential

for Mg^{2+} sensitivity. This result is consistent with E374 being part of the high-affinity Mg^{2+} binding site. Both Asp and Glu residues at position 374 are able to provide coordination for Mg^{2+} binding, whereas other residues, regardless of their size or hydrophobicity, destroy Mg^{2+} binding.

We also examined the effects of E399 mutations on the activation of mSlo1 channels. Fig. 3 shows the comparison of the WT mSlo1 activation with that of mutant channels E399R, E399D, E399N, E399Q, and E399W. Similar to E374, mutation of E399 to any amino acid other than Asp destroys Mg^{2+} sensitivity, indicating that the carboxylate on this residue is also essential for Mg^{2+} sensitivity. Multiple comparison with Tukey's test indicates that the result of E399D in Fig. 3 *C* is significantly different from the result of the other mutants (>95% confidence level).

Although Mg^{2+} sensitivity is retained in both E374D and E399D mutant channels, it is significantly reduced (Fig. 2, *B* and *C*, Fig. 3 *B* and *C*). In order to examine the Mg^{2+} sensitivity reduction in more detail, we measured *G-V* relations of E399D in various $[Mg^{2+}]_i$ between 0 and 100 mM at 0 $[Ca^{2+}]_i$ and fitted the data with Eq. 2 (Fig. 4 *A*):

$$P_o = \frac{1}{1 + L_0 \cdot e^{\frac{-zFV}{RT}} \cdot \left(\frac{1 + \frac{[Mg]}{K_{cM1}}}{1 + \frac{[Mg]}{K_{oM1}}} \right)^4 \cdot \left(\frac{1 + \frac{[Mg]}{K_{cM2}}}{1 + \frac{[Mg]}{K_{oM2}}} \right)^4}. \quad (2)$$

Equation 2 is derived from a model of mSlo1 activation by Mg^{2+} binding to the two different binding sites (63), where P_o is the open probability of the channel; L_0 is the equilibrium constant between the closed and open states at the voltage of 0 mV when no Ca^{2+} or Mg^{2+} is bound ($L_0 = [C_0]/[O_0]$); z is the number of equivalent gating charges; K_{cM1}, K_{cM2}, K_{oM1}, and K_{oM2} are the dissociation constants of Mg^{2+} binding to the high- and low-affinity Mg^{2+} sites on each subunit when the channel is at closed and open states, respectively; and *V, T, F*, and *R* have their usual meanings. Equation 2 does not include Ca^{2+}-dependent activation because $[Ca^{2+}]_i$ in these experiments is 0 (Fig. 4). We have demonstrated that the two Mg^{2+} binding sites act independently in channel activation, and mutations E399N and E374A:E399N do not affect channel activation through the low-affinity binding site (63). Such independence is further demonstrated in Fig. 4 *B*, which shows that for several other E399 mutations that also destroy Mg^{2+} sensitivity related to the high-affinity site, the shift of *G-V* relations in response to an increase of $[Mg^{2+}]_i$ from 10 to 100 mM is similar to that of WT mSlo1. Therefore, it is reasonable to assume that the low-affinity binding site is not affected by E399D either, and the parameters related to this binding site in Eq. 2 are the same as in the WT mSlo1 (Table 1). Comparing the parameters of model fitting to the WT and E399D data (Table 1), we find that Mg^{2+} affinity of the high-affinity binding site is altered by the mutation in both open and closed conformation (K_{oM1} and K_{cM1}). The model used in the fitting is derived from

TABLE 1 Parameters from MWC model fitting to activation data of the WT and mutant mSlo1 channels

	WT	E399D	Q397K	Q397E	Q397C
L_0	**9334**	**6857 ± 814**	**1492 ± 187**	**63,525 ± 1010**	**16,525 ± 1410**
z	1.25	1.25	1.25	1.25	1.25
K_{cM1} (mM)	**5.46**	**2.50 ± 0.78**	**6.90 ± 1.43**	**3.01 ± 0.20**	**4.47 ± 0.28**
K_{oM1} (mM)	**2.25**	**2.10 ± 0.65**	**4.99 ± 0.98**	**1.20 ± 0.07**	**2.50 ± 0.14**
K_{cM2} (mM)	136.1	136.1	136.1	136.1	136.1
K_{oM2} (mM)	40.1	40.1	40.1	40.1	40.1

Parameters for the WT channels were taken from Hu et al. (63); z, K_{cM2}, and K_{oM2} of the mutant channels are fixed to be the same as those of the WT channels. Bold values indicate the parameters that are different between the WT and mutant channels. ± indicates parameter mean ± SE.

the MWC model (39,64), in which Mg^{2+} binds to the open channel with higher affinity and shifts the closed-open equilibrium toward the open conformation by factor c ($c = K_{oM1}/K_{cM1}$) (64). Table 1 shows that in the open conformation, the affinity of Mg^{2+} binding may be unaffected by the mutation E399D (K_{oM1} similar), whereas in the closed conformation, the affinity may even be increased (K_{cM1} smaller). Thus, the

mutant channel has a larger c factor than the WT mSlo1, signifying that activation of the E399D channel is less sensitive to the effects of Mg^{2+} binding (Figs. 3 *C* and 4 *A*).

We then examined the effects of Q397 mutations on the activation of mSlo1 channels. Fig. 5 *A* shows the comparison of Mg^{2+}-dependent activation of the WT mSlo1 channels with that of mutant channels Q397R, Q397K, Q397D, Q397E, Q397C, and Q397W. Unlike mutations of E374 and E399, most of which abolish Mg^{2+} sensitivity, none of the mutations of Q397 destroys Mg^{2+} sensitivity entirely. Most surprisingly, even when the residue is mutated to positively charged side chains (Q397R and Q397K), the channel still
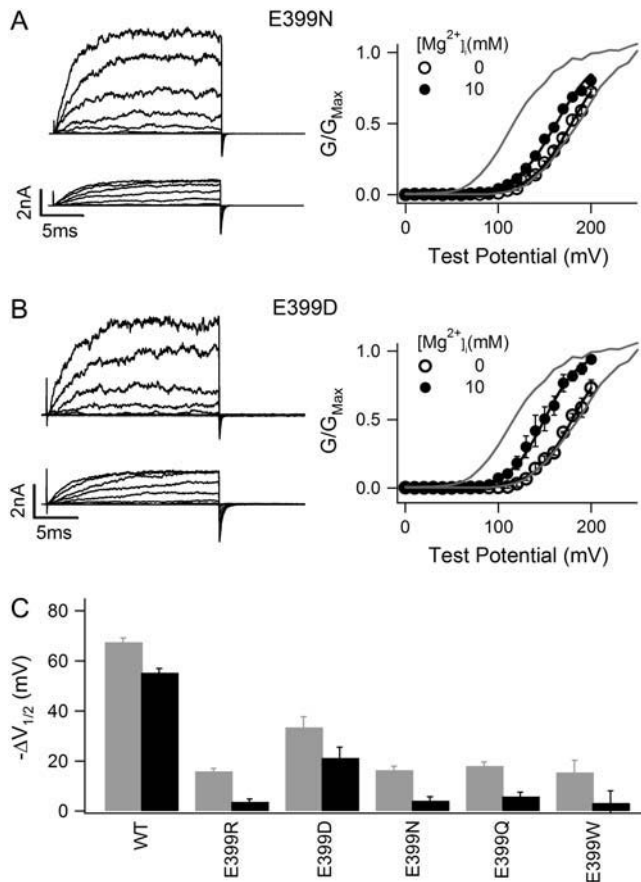

FIGURE 3 Effects of E399 mutations on Mg^{2+} sensitivity. (*A* and *B*) Mg^{2+}-dependent activation of E399N (*A*) and E399D (*B*) channels at 0 [Ca^{2+}]$_i$. (*Left panels*) Current traces recorded at 0 (*upper*) or 10 mM (*lower*) [Mg^{2+}]$_i$. Voltage protocols are similar as in Fig. 2, *A* and *B*. (*Right panels*) Mean *G-V* relations and fits with the Boltzmann relation (*solid lines*). Gray lines are *G-V* relations of WT mSlo1 channels for comparison. (*C*) *G-V* shift from 0 to 10 mM [Mg^{2+}]$_i$ at 0 [Ca^{2+}]$_i$ of WT mSlo1 and mutant channels. Gray and black bars have similar meanings as in Fig. 2 *C*.
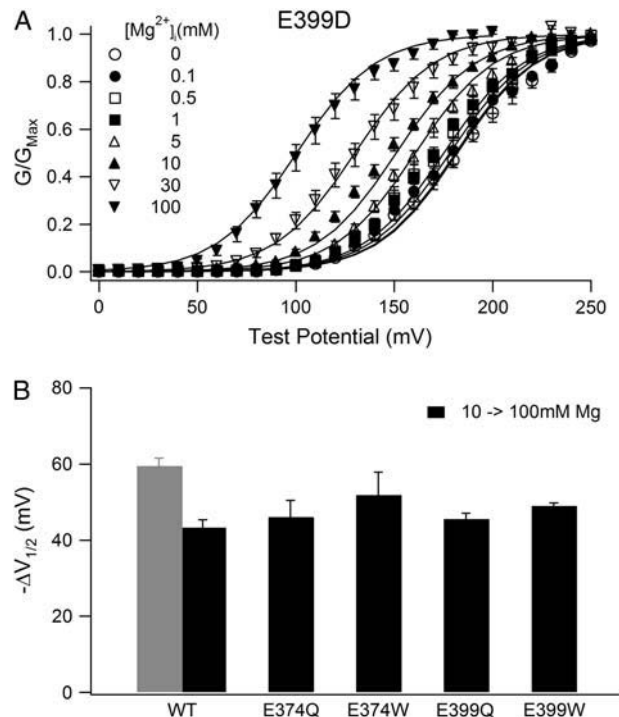
FIGURE 4 Effects of mutation E399D on Mg^{2+} binding. (*A*) Mean *G-V* relations of E399D mutant channels at 0 [Ca^{2+}]$_i$ and indicated [Mg^{2+}]$_i$. Solid lines are model fittings according to Eq. 2. The parameters obtained from the fitting are listed in Table 1. (*B*) *G-V* shifts from 10 to 100 mM [Mg^{2+}]$_i$ at 0 [Ca^{2+}]$_i$ of WT mSlo1 and mutant channels. For WT mSlo1 channels, the gray bar is data measured in experiments, and the black bar is the experimental data subtracted by the amount of *G-V* shift (−16.2 mV) caused by Mg^{2+} binding to the high-affinity Mg^{2+} site.
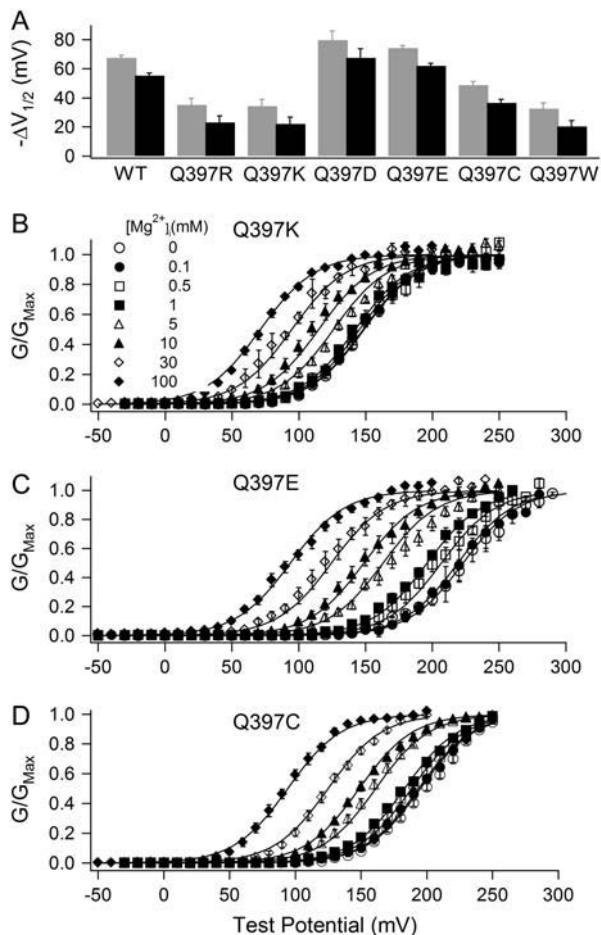
FIGURE 5 Effects of Q397 mutations on Mg^{2+} sensitivity of channel activation and on Mg^{2+} binding. (A) G-V shifts from 0 to 10 mM $[Mg^{2+}]_i$ at 0 $[Ca^{2+}]_i$ of WT mSlo1 and mutant channels. Gray and black bars have similar meanings as in Fig. 2 C. (B–D) Mean G-V relations of mutant channels Q397K (B), Q397E (C), and Q397C (D) at 0 $[Ca^{2+}]_i$ and indicated $[Mg^{2+}]_i$. Solid lines are model fittings according to Eq. 2. The parameters obtained from the fitting are listed in Table 1.

retains Mg^{2+} sensitivity (Fig. 5 A). These results are not consistent with the idea that the side chain of Q397 is the ligand for the Mg^{2+} binding site. Nevertheless, the results in Fig. 5 A suggest that because the side chain of Q397 is spatially close to E374 and E399, the mutations of Q397 may affect Mg^{2+} binding if E374 and E399 are part of the Mg^{2+} binding site, and thus the Mg^{2+} sensitivity of channel activation. Mutations Q397R, Q397K, Q397C, and Q397W reduce Mg^{2+} sensitivity of the channel significantly (Fig. 5 A). On the other hand, when Q397 is mutated to negatively charged side chains (Q397E and Q397D), Mg^{2+} sensitivity is increased (Fig. 5 A). We also measured the G-V relations of Q397C, Q397K, and Q397E mutant channels at various $[Mg^{2+}]_i$ levels between 0 and 100 mM at 0 $[Ca^{2+}]_i$, and fitted the data with Eq. 2 (Fig. 5, B–D). The parameters obtained from model fittings are listed in Table 1. Compared to the WT mSlo1 channels, these mutations altered Mg^{2+} affinity in

both the closed and the open conformations of the channel (K_{cM1} and K_{oM1}), resulting in a smaller c factor ($c = K_{oM1}/K_{cM1}$) and an increased Mg^{2+} sensitivity in the case of Q397E and in a larger c factor and a reduced Mg^{2+} sensitivity in the case of Q397K and Q397C (Fig. 5 and Table 1).

The increase of Mg^{2+} sensitivity by mutations Q397D and Q397E suggests that a negative charge at position 397 may affect Mg^{2+} binding by an electrostatic attraction to the bound Mg^{2+} ion. If this is the case, a positive charge at this position is expected to reduce Mg^{2+} sensitivity by electrical repulsion. Our experiment results show that mutations Q397R and Q397K indeed reduced Mg^{2+} sensitivity (Fig. 5, A and B). However, both Q397C and Q397W also reduced Mg^{2+} sensitivity (Fig. 5 A), suggesting that a conformational change caused by Q397 mutations may also be important to Mg^{2+} binding. Therefore, it is not clear whether the effect of Q397R and Q397K was caused by an electrostatic interaction or a conformational change. To address this question, we treated Q397C with the Cys-modifying reagent MTSET(+). The covalent addition of a positively charged MTSET(+) to Q397C had no apparent effect on the kinetics of channel gating (Fig. 6 A), but it reduced Mg^{2+} sensitivity as compared to Q397C before MTSET(+) treatment (Fig. 6 B). These experiments were performed on the double mutation Q397C:C430A to eliminate the effect of MTSET(+) modification of the native C430 (65). C430A alone does
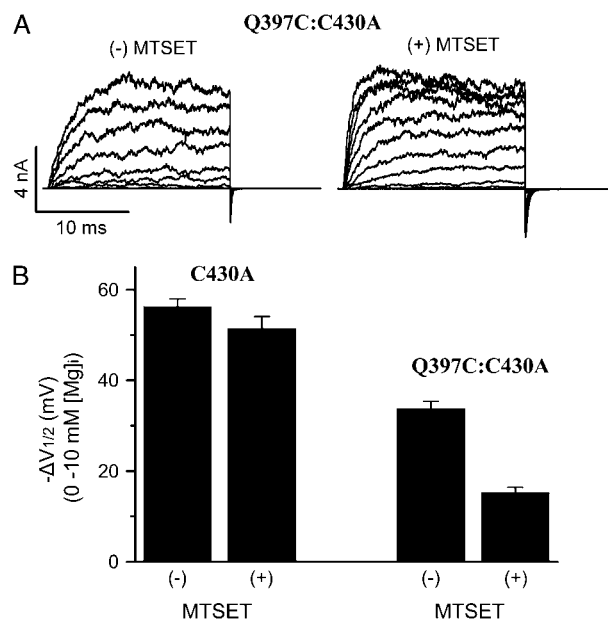

FIGURE 6 MTSET(+) modification of Q397C reduces Mg^{2+} sensitivity of channel activation. (A) Current traces of Q397C:C430A mutant channels recorded at 0 $[Mg^{2+}]_i$ and 0 $[Ca^{2+}]_i$ before (left) and after (right) MTSET(+) treatment. (B) G-V shifts of C430A and Q397C:C430A mutant channels from 0 to 10 mM $[Mg^{2+}]_i$ at 0 $[Ca^{2+}]_i$ before and after MTSET(+) treatment. The G-V shifts are subtracted by the amount of G-V shift (-12.2 mV) caused by Mg^{2+} binding to the low-affinity Mg^{2+} site.

not alter Mg^{2+} sensitivity of the channel, and MTSET(+) treatment of C430A has no effect on Mg^{2+} sensitivity either (Fig. 6 B), indicating that the effects of MTSET(+) on Q397C:C430A are specifically caused by the modification of Q397C. Fig. 6 B shows that Q397C reduces Mg^{2+} sensitivity in the background of C430A (10 mM Mg^{2+} resulted in a shift of the G-V relation -47.76 ± 1.59 mV for Q397C: C430A channels as compared to -70.28 ± 1.68 mV for C430A), which is similar to its effect on the WT mSlo1 (Fig. 5 A). The modification of Q397C by MTSET(+) further reduces Mg^{2+} sensitivity, supporting the mechanism that electric charges at position 397 may affect Mg^{2+} sensitivity by an electrostatic interaction with the bound Mg^{2+} ion.

DISCUSSION

We examined the mechanism of Mg^{2+}-dependent activation of mSlo1 BK channels by studying the effects of mutating E374, E399, and Q397. We found that a carboxylate, or a negative charge, on the side chain of residues 374 and 399 is essential for Mg^{2+} sensitivity (Figs. 2 and 3). On the other hand, no mutations of Q397 abolished Mg^{2+} sensitivity, suggesting that the side chain of Q397 may not coordinate to Mg^{2+} (Fig. 5). However, Q397 is spatially close to E374 and E399 (Fig. 1), so the effects of Q397 mutations may derive from their interference with Mg^{2+} binding if E374 and E399 indeed form the binding site (Fig. 1). Effects of Q397 mutations and chemical modification of Q397C suggest that the mutations affect Mg^{2+} binding by altering the conformation of the binding site as well as by electrostatic interactions with the bound Mg^{2+} ion (Figs. 5 and 6; Table 1).

Based on the homology between Slo1 channels and the K$^+$ channels in *E. coli* or MthK, E374, E399, and Q397 are located on the surface of a Rossman fold (38,58,59). The relation of these residues is comparable to the organization of the Mg^{2+} binding site in the response regulator of bacterial chemotaxis, CheY, which is also located on the surface of a Rossman fold, and the bound Mg^{2+} ion is coordinated by the side-chain carboxylates of two Asp residues (D13 and D57), the backbone carbonyl of Asn-59, and three water molecules (66–68). In mSlo1, mutations of E374 and E399 even to amino acids with an oxygen-containing side chain abolish Mg^{2+} sensitivity as long as the substituting residue is not an Asp (Figs. 2 and 3). Similarly, mutations D13N and D57N of the CheY's Mg^{2+} binding site reduce Mg^{2+} affinity by more than an order of magnitude (69). In addition, the Mg^{2+} binding sites in mSlo1 or CheY do not discriminate between metals on the basis of their size. For example, the dissociation constants of Mg^{2+} and Ca^{2+} binding to mSlo1 at the open state are 2.2–6.0 mM and 0.66 mM, respectively (37,39,63), whereas the dissociation constants of Mg^{2+} and Ca^{2+} binding to CheY are 1.0 mM and 0.4 mM, respectively (70). Such a lack of size specificity is in striking contrast to the dissociation constants of Mg^{2+} and Ca^{2+} binding to the high-affinity Ca^{2+} binding site of mSlo1 at the open state,

which are 4.73–5.6 mM and 0.75–1.3 μM, respectively (37,39,63,64,71). These properties of the Mg^{2+} binding site in CheY derive from its coordination scheme in which one hemisphere of the bound ion is coordinated by three protein oxygens, and the other hemisphere is coordinated by three solvent molecules at the protein surface (70). On one hand, the flexible solvent shell can easily vary its coordination number and shape to accommodate bound ions of different sizes; on the other hand, the side-chain carboxylates are required to provide strong coordination (72). Because the Mg^{2+} binding site in mSlo1 shares the same properties as that in CheY, it may also share a similar coordination scheme, i.e., the two side-chain carboxylates from E374 and E399 and the main-chain carbonyl at Q397 provide oxygens for Mg^{2+} coordination (38), whereas the side chain of Q397 may not be part of the ligands for the Mg^{2+} binding site in mSlo1 (Fig. 5). According to this coordination scheme, although mutations E374D and E399D may cause conformational changes of the binding site, the channel retains Mg^{2+} sensitivity because the flexible solvent shell may vary to accommodate such conformational changes to allow Mg^{2+} binding.

Mg^{2+} activates the BK channel by an allosteric mechanism (Fig. 1) (37–40,63); i.e., Mg^{2+} binding induces a conformational change of the channel protein that eventually opens the activation gate distant from the Mg^{2+} binding site. In CheY, Mg^{2+} binding induces a conformational change near the binding site (67,68,73). Conformational changes near the binding site are also observed in many other proteins as a result of metal binding (74–77). In mSlo1, Q397 is close to E374 and E399 (Fig. 1). Because all mutations of Q397 in our study affect Mg^{2+} sensitivity, this residue is likely involved in the Mg^{2+}-dependent activation mechanism such that the Mg^{2+} binding induces conformational changes at and around Q397, and reciprocally, Mg^{2+} binding is also altered by the mutations of Q397.

However, it is hard for a simple conformational change to explain the results that Q397D and Q397E increase Mg^{2+} sensitivity whereas other mutations reduce Mg^{2+} sensitivity (Fig. 5 A). When the chemical properties of the substituting side chains of Q397 mutations are compared with their effects on Mg^{2+} sensitivity, it is clear that the side-chain size (Van der Waals volume: W > R > E > K $\geq$ Q > D > C) or hydrophobicity (C > W > Q > K > E > D > R) (78) may not decide the effects of mutations on Mg^{2+} sensitivity (E $\approx$ D > Q > C > W $\approx$ R $\approx$ K) (Fig. 5 A). On the other hand, it is apparent that both Q397E and Q397D contain a negative charge, and both increase Mg^{2+} sensitivity. When Q397C is modified by MTSET(+), the covalently attached positive charge reduces Mg^{2+} sensitivity, similar to the effects of mutations Q397R and Q397K (Figs. 5 and 6). Thus, electrostatic interaction plays an important role in the effect of Q397 mutations. The charge introduced to the residue at 397 by mutations affects Mg^{2+} binding by either electrical repulsion or attraction to the bound Mg^{2+} ion. Consistent with this mechanism, fittings of the MWC model to G-V relations

at various $[Mg^{2+}]_i$ suggest that Q397K reduces Mg^{2+} affinity in both the closed and the open conformations of the channel (K_{cM1} and K_{oM1} become larger), whereas Q397E increases Mg^{2+} affinity (K_{cM1} and K_{oM1} become smaller) (Table 1). Such an electrostatic contribution to metal binding by charged surface residues has been reported previously and has been suggested as a common mechanism in metal-binding proteins (79–82). The electrostatic interaction between Q397 mutations and the Mg^{2+} binding site suggests that Q397 is located close to the Mg^{2+} binding site, further supporting that E374 and E399 are the ligands for the Mg^{2+} binding site.

In conclusion, this study further demonstrates that E374 and E399 side chains are part of the Mg^{2+} binding site. Mg^{2+} sensitivity of channel activation can be tuned by altering Mg^{2+} binding through changing the conformation of the binding site per se (E374D and E399D) or the environment of the binding site (Q397 mutations). However, the effect of Q397 mutations on Mg^{2+}-dependent activation requires a functional Mg^{2+} binding site because a double mutation, E374A:Q397E, had no Mg^{2+} sensitivity (data not shown). This result also demonstrates that although Q397 is close to the Mg^{2+} binding site, within the range of electrostatic interactions, it cannot replace E374 in coordination of Mg^{2+} binding.

REFERENCES

1. Lewis, R. S., and A. J. Hudspeth. 1983. Voltage- and ion-dependent conductances in solitary vertebrate hair cells. *Nature.* 304:538–541.

2. Magleby, K. L., and B. S. Pallotta. 1983. Calcium dependence of open and shut interval distributions from calcium-activated potassium channels in cultured rat muscle. *J. Physiol.* 344:585–604.

3. Magleby, K. L., and B. S. Pallotta. 1983. Burst kinetics of single calcium-activated potassium channels in cultured rat muscle. *J. Physiol.* 344:605–623.

4. Petersen, O. H., and Y. Maruyama. 1984. Calcium-activated potassium channels and their role in secretion. *Nature.* 307:693–696.

5. Storm, J. F. 1987. Action potential repolarization and a fast after-hyperpolarization in rat hippocampal pyramidal cells. *J. Physiol. (Lond.).* 385:733–759.

6. Lancaster, B., R. A. Nicoll, and D. J. Perkel. 1991. Calcium activates two types of potassium channels in rat hippocampal neurons in culture. *J. Neurosci.* 11:23–30.

7. McManus, O. B. 1991. Calcium-activated potassium channels: regulation by calcium. *J. Bioenerg. Biomembr.* 23:537–560.

8. Brayden, J. E., and M. T. Nelson. 1992. Regulation of arterial tone by activation of calcium-dependent potassium channels. *Science.* 256:532–535.

9. Bielefeldt, K., and M. B. Jackson. 1993. A calcium-activated potassium channel causes frequency-dependent action-potential failures in a mammalian nerve terminal. *J. Neurophysiol.* 70:284–298.

10. Crest, M., and M. Gola. 1993. Large conductance Ca^{2+}-activated K^+ channels are involved in both spike shaping and firing regulation in *Helix* neurones. *J. Physiol.* 465:265–287.

11. Robitaille, R., M. L. Garcia, G. J. Kaczorowski, and M. P. Charlton. 1993. Functional colocalization of calcium and calcium-gated potassium channels in control of transmitter release. *Neuron.* 11:645–655.

12. Yazejian, B., D. A. DiGregorio, J. L. Vergara, R. E. Poage, S. D. Meriney, and A. D. Grinnell. 1997. Direct measurements of presynaptic calcium and calcium-activated potassium currents regulating neurotransmitter release at cultured *Xenopus* nerve-muscle synapses. *J. Neurosci.* 17:2990–3001.

13. Marrion, N. V., and S. J. Tavalin. 1998. Selective activation of Ca^{2+}-activated K^+ channels by co-localized Ca^{2+} channels in hippocampal neurons. *Nature.* 395:900–905.

14. Safronov, B. V., and W. Vogel. 1998. Large conductance Ca^{2+}-activated K^+ channels in the soma of rat motoneurones. *J. Membr. Biol.* 162:9–15.

15. Nelson, M. T., and J. M. Quayle. 1995. Physiological roles and properties of potassium channels in arterial smooth muscle. *Am. J. Physiol.* 268:C799–C822.

16. Adams, P. R., A. Constanti, D. A. Brown, and R. B. Clark. 1982. Intracellular Ca^{2+} activates a fast voltage-sensitive K^+ current in vertebrate sympathetic neurones. *Nature.* 296:746–749.

17. Lancaster, B., and R. A. Nicoll. 1987. Properties of two calcium-activated hyperpolarizations in rat hippocampal neurones. *J. Physiol. (Lond.).* 389:187–203.

18. Roberts, W. M., R. A. Jacobs, and A. J. Hudspeth. 1990. Colocalization of ion channels involved in frequency selectivity and synaptic transmission at presynaptic active zones of hair cells. *J. Neurosci.* 10:3664–3684.

19. Robitaille, R., and M. P. Charlton. 1992. Presynaptic calcium signals and transmitter release are modulated by calcium-activated potassium channels. *J. Neurosci.* 12:297–305.

20. Wellman, G. C., and M. T. Nelson. 2003. Signaling between SR and plasmalemma in smooth muscle: sparks and the activation of Ca^{2+}-sensitive ion channels. *Cell Calcium.* 34:211–229.

21. Tanaka, Y., M. Aida, H. Tanaka, K. Shigenobu, and L. Toro. 1998. Involvement of maxi-K_{Ca} channel activation in atrial natriuretic peptide-induced vasorelaxation. *Naunyn Schmiedebergs Arch. Pharmacol.* 357:705–708.

22. Perez, G. J., A. D. Bonev, J. B. Patlak, and M. T. Nelson. 1999. Functional coupling of ryanodine receptors to K_{Ca} channels in smooth muscle cells from rat cerebral arteries. *J. Gen. Physiol.* 113:229–238.

23. Pluger, S., J. Faulhaber, M. Furstenau, M. Lohn, R. Waldschutz, M. Gollasch, H. Haller, F. C. Luft, H. Ehmke, and O. Pongs. 2000. Mice with disrupted BK channel beta1 subunit gene feature abnormal Ca^{2+} spark/STOC coupling and elevated blood pressure. *Circ. Res.* 87:E53–E60.

24. Wu, Y. C., J. J. Art, M. B. Goodman, and R. Fettiplace. 1995. A kinetic description of the calcium-activated potassium channel and its application to electrical tuning of hair cells. *Prog. Biophys. Mol. Biol.* 63:131–158.

25. Rosenblatt, K. P., Z. P. Sun, S. Heller, and A. J. Hudspeth. 1997. Distribution of Ca^{2+}-activated K^+ channel isoforms along the tonotopic gradient of the chicken's cochlea. *Neuron.* 19:1061–1075.

26. Hudspeth, A. J., and R. S. Lewis. 1988. Kinetic analysis of voltage- and ion-dependent conductances in saccular hair cells of the bull-frog, *Rana catesbeiana. J. Physiol. (Lond.).* 400:237–274.

27. Fettiplace, R., and P. A. Fuchs. 1999. Mechanisms of hair cell tuning. *Annu. Rev. Physiol.* 61:809–834.

28. Ahluwalia, J., A. Tinker, L. H. Clapp, M. R. Duchen, A. Y. Abramov, S. Pope, M. Nobles, and A. W. Segal. 2004. The large-conductance

Ca^{2+}-activated K$^+$ channel is essential for innate immunity. *Nature.* 427:853–858.

29. Squire, L. G., and O. H. Petersen. 1987. Modulation of Ca^{2+}- and voltage-activated K$^+$ channels by internal Mg^{2+} in salivary acinar cells. *Biochim. Biophys. Acta.* 899:171–175.

30. Zamoyski, V. L., V. N. Serebryakov, and R. Schubert. 1989. Activation and blocking effects of divalent cations on the calcium-dependent potassium channel of high conductance. *Biomed. Biochim. Acta.* 48:S388–S392.

31. Ferguson, W. B. 1991. Competitive Mg^{2+} block of a large-conductance, Ca^{2+}-activated K$^+$ channel in rat skeletal muscle. Ca^{2+}, Sr^{2+}, and Ni^{2+} also block. *J. Gen. Physiol.* 98:163–181.

32. McLarnon, J. G., and D. Sawyer. 1993. Effects of divalent cations on the activation of a calcium-dependent potassium channel in hippocampal neurons. *Pflugers Arch.* 424:1–8.

33. Zhang, X., E. Puil, and D. A. Mathers. 1995. Effects of intracellular Mg^{2+} on the properties of large-conductance, Ca^{2+}-dependent K$^+$ channels in rat cerebrovascular smooth muscle cells. *J. Cereb. Blood Flow Metab.* 15:1066–1074.

34. Morales, E., W. C. Cole, C. V. Remillard, and N. Leblane. 1996. Block of large conductance Ca^{2+}-activated K$^+$ channels in rabbit vascular myocytes by internal Mg^{2+} and Na$^+$. *J. Physiol.* 495:701–716.

35. Wachter, C., and K. Turnheim. 1996. Inhibition of high-conductance, calcium-activated potassium channels of rabbit colon epithelium by magnesium. *J. Membr. Biol.* 150:275–282.

36. Bringmann, A., F. Faude, and A. Reichenbach. 1997. Mammalian retinal glial (Muller) cells express large-conductance Ca^{2+}-activated K$^+$ channels that are modulated by Mg^{2+} and pH and activated by protein kinase A. *Glia.* 19:311–323.

37. Zhang, X., C. R. Solaro, and C. J. Lingle. 2001. Allosteric regulation of BK channel gating by Ca^{2+} and Mg^{2+} through a nonselective, low affinity divalent cation site. *J. Gen. Physiol.* 118:607–636.

38. Shi, J., G. Krishnamoorthy, Y. Yang, L. Hu, N. Chaturvedi, D. Harilal, J. Qin, and J. Cui. 2002. Mechanism of magnesium activation of calcium-activated potassium channels. *Nature.* 418:876–880.

39. Shi, J., and J. Cui. 2001. Intracellular Mg^{2+} enhances the function of BK-type Ca^{2+} activated K$^+$ channels. *J. Gen. Physiol.* 118:589–606.

40. Xia, X. M., X. Zeng, and C. J. Lingle. 2002. Multiple regulatory sites in large-conductance calcium-activated potassium channels. *Nature.* 418:880–884.

41. Altura, B. M., B. T. Altura, A. Carella, A. Gebrewold, T. Murakawa, and A. Nishio. 1987. Mg^{2+}-Ca^{2+} interaction in contractility of vascular smooth muscle: Mg^{2+} versus organic calcium channel blockers on myogenic tone and agonist- induced responsiveness of blood vessels. *Can. J. Physiol. Pharmacol.* 65:729–745.

42. Altura, B. M., and R. K. Gupta. 1992. Cocaine induces intracellular free Mg deficits, ischemia and stroke as observed by in-vivo ^{31}P-NMR of the brain. *Biochim. Biophys. Acta.* 1111:271–274.

43. Matsuda, H., A. Saigusa, and H. Irisawa. 1987. Ohmic conductance through the inwardly rectifying K channel and blocking by internal Mg^{2+}. *Nature.* 325:156–159.

44. Vandenberg, C. A. 1987. Inward rectification of a potassium channel in cardiac ventricular cells depends on internal magnesium ions. *Proc. Natl. Acad. Sci. USA.* 84:2560–2564.

45. White, R. E., and H. C. Hartzell. 1988. Effects of intracellular free magnesium on calcium current in isolated cardiac myocytes. *Science.* 239:778–780.

46. Chuang, H., Y. N. Jan, and L. Y. Jan. 1997. Regulation of IRK3 inward rectifier K$^+$ channel by m$_1$ acetylcholine receptor and intracellular magnesium. *Cell.* 89:1121–1132.

47. Romani, A. M., V. D. Matthews, and A. Scarpa. 2000. Parallel stimulation of glucose and Mg^{2+} accumulation by insulin in rat hearts and cardiac ventricular myocytes. *Circ. Res.* 86:326–333.

48. Vink, R., and I. Cernak. 2000. Regulation of intracellular free magnesium in central nervous system injury. *Front. Biosci.* 5:D656–D665.

49. Laurant, P., and R. M. Touyz. 2000. Physiological and pathophysiological role of magnesium in the cardiovascular system: implications in hypertension. *J. Hypertens.* 18:1177–1191.

50. Seelig, M. S. 2000. Interrelationship of magnesium and congestive heart failure. *Wien. Med. Wochenschr.* 150:335–341.

51. Atkinson, N. S., G. A. Robertson, and B. Ganetzky. 1991. A component of calcium-activated potassium channels encoded by the *Drosophila* slo locus. *Science.* 253:551–555.

52. Adelman, J. P., K. Z. Shen, M. P. Kavanaugh, R. A. Warren, Y. N. Wu, A. Lagrutta, C. T. Bond, and R. A. North. 1992. Calcium-activated potassium channels expressed from cloned complementary DNAs. *Neuron.* 9:209–216.

53. Butler, A., S. Tsunoda, D. P. McCobb, A. Wei, and L. Salkoff. 1993. *mSlo*, a complex mouse gene encoding ''maxi'' calcium-activated potassium channels. *Science.* 261:221–224.

54. Dworetzky, S. I., J. T. Trojnacki, and V. K. Gribkoff. 1994. Cloning and expression of a human large-conductance calcium-activated potassium channel. *Brain Res. Mol. Brain Res.* 27:189–193.

55. Tseng-Crank, J., C. D. Foster, J. D. Krause, R. Mertz, N. Godinot, T. J. DiChiara, and P. H. Reinhart. 1994. Cloning, expression, and distribution of functionally distinct Ca^{2+}-activated K$^+$ channel isoforms from human brain. *Neuron.* 13:1315–1330.

56. Pallanck, L., and B. Ganetzky. 1994. Cloning and characterization of human and mouse homologs of the *Drosophila* calcium-activated potassium channel gene, *slowpoke. Hum. Mol. Genet.* 3:1239–1243.

57. Magleby, K. L. 2003. Gating mechanism of BK (Slo1) channels: so near, yet so far. *J. Gen. Physiol.* 121:81–96.

58. Jiang, Y., A. Lee, J. Chen, M. Cadene, B. T. Chait, and R. MacKinnon. 2002. Crystal structure and mechanism of a calcium-gated potassium channel. *Nature.* 417:515–522.

59. Jiang, Y., A. Pico, M. Cadene, B. T. Chait, and R. MacKinnon. 2001. Structure of the RCK domain from the *E. coli* K$^+$ channel and demonstration of its presence in the human BK channel. *Neuron.* 29:593–601.

60. Cui, J., D. H. Cox, and R. W. Aldrich. 1997. Intrinsic voltage dependence and Ca^{2+} regulation of mslo large conductance Ca-activated K$^+$ channels. *J. Gen. Physiol.* 109:647–673.

61. Delano, W. L. 2002. The Pymol molecular graphics system. Delano Scientific, San Carlos, CA.. http://www.pymol.org. [Online].

62. Guex, N., and M. C. Peitsch. 1997. SWISS-MODEL and the Swiss-PdbViewer: an environment for comparative protein modeling. *Electrophoresis.* 18:2714–2723.

63. Hu, L., H. Yang, J. Shi, and J. Cui. 2006. Effects of multiple metal binding sites on calcium and magnesium-dependent activation of BK channels. *J. Gen. Physiol.* 127:35–50.

64. Cox, D. H., J. Cui, and R. W. Aldrich. 1997. Allosteric gating of a large conductance Ca-activated K$^+$ channel. *J. Gen. Physiol.* 110:257–281.

65. Zhang, G., and F. T. Horrigan. 2005. Cysteine modification alters voltage- and Ca^{2+}-dependent gating of large conductance (BK) potassium channels. *J. Gen. Physiol.* 125:213–236.

66. Stock, J. B., M. G. Surette, W. R. McCleary, and A. M. Stock. 1992. Signal transduction in bacterial chemotaxis. *J. Biol. Chem.* 267:19753–19756.

67. Bellsolell, L., J. Prieto, L. Serrano, and M. Coll. 1994. Magnesium binding to the bacterial chemotaxis protein CheY results in large conformational changes involving its functional surface. *J. Mol. Biol.* 238:489–495.

68. Stock, A. M., E. Martinez-Hackert, B. F. Rasmussen, A. H. West, J. B. Stock, D. Ringe, and G. A. Petsko. 1993. Structure of the Mg^{2+}-bound form of CheY and mechanism of phosphoryl transfer in bacterial chemotaxis. *Biochemistry.* 32:13375–13380.

69. Lukat, G. S., A. M. Stock, and J. B. Stock. 1990. Divalent metal ion binding to the CheY protein and its significance to phosphotransfer in bacterial chemotaxis. *Biochemistry.* 29:5436–5442.

70. Needham, J. V., T. Y. Chen, and J. J. Falke. 1993. Novel ion specificity of a carboxylate cluster Mg(II) binding site: strong charge selectivity and weak size selectivity. *Biochemistry.* 32:3363–3367.

71. Horrigan, F. T., and R. W. Aldrich. 2002. Coupling between voltage sensor activation, Ca^{2+} binding and channel opening in large conductance (BK) potassium channels. *J. Gen. Physiol.* 120:267–305.

72. Dudev, T., and C. Lim. 2003. Principles governing Mg, Ca, and Zn binding and selectivity in proteins. *Chem. Rev.* 103:773–788.

73. Falke, J. J., R. B. Bass, S. L. Butler, S. A. Chervitz, and M. A. Danielson. 1997. The two-component signaling pathway of bacterial chemotaxis: a molecular view of signal transduction by receptors, kinases, and adaptation enzymes. *Annu. Rev. Cell Dev. Biol.* 13:457–512.

74. Babu, C. S., T. Dudev, R. Casareno, J. A. Cowan, and C. Lim. 2003. A combined experimental and theoretical study of divalent metal ion selectivity and function in proteins: application to *E. coli* ribonuclease H1. *J. Am. Chem. Soc.* 125:9318–9328.

75. Lewit-Bentley, A., and S. Rety. 2000. EF-hand calcium-binding proteins. *Curr. Opin. Struct. Biol.* 10:637–643.

76. Ikura, M. 1996. Calcium binding and conformational response in EF-hand proteins. *Trends Biochem. Sci.* 21:14–17.

77. Nelson, M. R., and W. J. Chazin. 1998. An interaction-based analysis of calcium-induced conformational changes in Ca^{2+} sensor proteins. *Protein Sci.* 7:270–282.

78. Creighton, T. E. 1992. *Proteins: Structures and Molecular Principles.* New York: W.H. Freeman.

79. Linse, S., P. Brodin, C. Johansson, E. Thulin, T. Grundstrom, and S. Forsen. 1988. The role of protein surface charges in ion binding. *Nature.* 335:651–652.

80. Linse, S., C. Johansson, P. Brodin, T. Grundstrom, T. Drakenberg, and S. Forsen. 1991. Electrostatic contributions to the binding of Ca^{2+} in calbindin D9k. *Biochemistry.* 30:154–162.

81. Sheng, J.-Z., A. Weljie, L. Sy, S. Ling, H. J. Vogel, and A. P. Braun. 2005. Homology modeling identifies C-terminal residues that contribute to the Ca^{2+} sensitivity of a BK_{Ca} channel. *Biophys. J.* 89:3079–3092.

82. Bao, L., C. Kaldany, E. C. Holmstrand, and D. H. Cox. 2004. Mapping the BK_{Ca} channel's ''Ca^{2+} bowl'': side-chains essential for Ca^{2+} sensing. *J. Gen. Physiol.* 123:475–489.